Brain, Behavior, and Immunity 122 (2024) 444–455

Contents lists available at ScienceDirect

Brain Behavior and Immunity

journal homepage: www.elsevier.com/locate/ybrbi

Full-length Article

CD8$^+$ T cells exacerbate AD-like symptoms in mouse model of amyloidosis

Xin Wang [a,1], Britney Campbell [a,1], Monica Bodogai [a,1], Ross A. McDevitt [b], Anton Patrikeev [c], Fedor Gusev [c], Emeline Ragonnaud [a], Konda Kumaraswami [a], Sophie Shirenova [d,e,f], Karin Vardy [d,e,f], Mohamed-Gabriel Alameh [g], Drew Weissman [g], Hellen Ishikawa-Ankerhold [h,i], Eitan Okun [d,e,f], Evgeny Rogaev [c], Arya Biragyn [a,*]

[a] Immunoregulation Section, Laboratory of Molecular Biology and Immunolgy, USA
[b] Mouse Phenotyping Unit, Comparative Medicine Section, National Institute on Aging, Baltimore, MD, USA
[c] Department of Psychiatry, University of Massachusetts Medical School, Worcester, MA, USA
[d] The Leslie and Susan Gonda Multidisciplinary Brain Research Center, Israel
[e] The Mina and Everard Goodman Faculty of Life Sciences, Israel
[f] The Paul Feder Laboratory on Alzheimer's Disease Research, Bar-Ilan University, Ramat Gan, Israel
[g] Institute of RNA Innovation, University of Pennsylvania, Philadelphia, PA, USA
[h] Department of Medicine I, University Hospital, Ludwig-Maximilians-Universität München, Munich, Germany
[i] Institute of Surgical Research at the Walter Brendel Centre of Experimental Medicine, University Hospital, LMU Munich, Munich, Germany

ARTICLE INFO

Keywords:
Aβ response
CD8$^+$ T cells
B cells
Alzheimer's disease
Amyloidosis

ABSTRACT

Alzheimer's disease (AD) is linked to toxic Aβ plaques in the brain and activation of innate responses. Recent findings however suggest that the disease may also depend on the adaptive immunity, as B cells exacerbate and CD8$^+$ T cells limit AD-like pathology in mouse models of amyloidosis. Here, by artificially blocking or augmenting CD8$^+$ T cells in the brain of 5xFAD mice, we provide evidence that AD-like pathology is promoted by pathogenic, proinflammatory cytokines and exhaustion markers expressing CXCR6$^+$ CD39$^+$CD73$^{+/-}$ CD8$^+$ T_{RM}-like cells. The CD8$^+$ T cells appear to act by targeting disease associated microglia (DAM), as we find them in tight complexes with microglia around Aβ plaques in the brain of mice and humans with AD. We also report that these CD8$^+$ T cells are induced by B cells in the periphery, further underscoring the pathogenic importance of the adaptive immunity in AD. We propose that CD8$^+$ T cells and B cells should be considered as therapeutic targets for control of AD, as their ablation at the onset of AD is sufficient to decrease CD8$^+$ T cells in the brain and block the amyloidosis-linked neurodegeneration.

1. Introduction

According to the prevailing Amyloid cascade hypothesis, Alzheimer's disease (AD) is caused by decades-long deposition of neurotoxic amyloid β-peptide aggregates (Aβ plaques) in the brain (Glenner and Wong, 1984). It leads to a chain of pathological events, including tauopathy, astrogliosis, accumulation of disease associated microglia (DAM), synaptic and neuronal dysfunction, and eventually dementia (Mattson, 2004). The process also involves activated peripheral innate immune cells (Baik et al., 2014; Zenaro et al., 2015), while the role of adaptive immunity remains poorly explored and is thought to be negligible (Prinz and Priller, 2014) despite the ability of aberrantly expressed brain antigens to drain into the deep cervical lymph nodes (cLN) (Da Mesquita et al., 2018) and induce T and B cells, as noted in multiple sclerosis (Goverman, 2009; Stern et al., 2014). B cells are mostly known for production of beneficial antibodies, which is used to ameliorate amyloid burden and memory decline in transgenic 3xTgAD, APP/PS1, and 5xFAD mice (the models of early-onset of AD; express differing copy numbers of human mutant APP and PSEN genes of familial AD (Gotz et al., 2018; Oakley et al., 2006)) (Bombois et al., 2007; Olkhanud et al., 2012) and in humans with mild cognitive impairment (MCI) in the recent phase 3 Clarity clinical trial (NCT03887455) (van Dyck et al., 2023). Even non-specific immunoglobulin appears to activate beneficial microglial phagocytosis in the brain (Marsh et al., 2016). Recently, we reported that AD surprisingly requires B cells to progress, as their depletion blocks the manifestation of Aβ-induced AD-like

* Corresponding author at: at: National Institute on Aging, 251 Bayview Blvd, Suite 100, Baltimore, MD 21224, USA.
E-mail address: biragyna@mail.nih.gov (A. Biragyn).
[1] Equal contribution

https://doi.org/10.1016/j.bbi.2024.08.045
Received 1 May 2024; Received in revised form 1 August 2024; Accepted 22 August 2024
Available online 25 August 2024
0889-1591/Published by Elsevier Inc.

symptoms in 5xFAD, APP/PS1 and 3xTgAD mice (Kim et al., 2021). The mechanism through which B cells promote AD is unknown, although we proposed that it is through activation of DAM. The B cell loss at the onset of AD is sufficient to decrease DAM and to restore homeostatic TGFβ$^+$ microglia (Kim et al., 2021). AD patients and elderly people can also increase Aβ-specific CD4$^+$ T cells in the circulation (Monsonego et al., 2003). CD4$^+$ T cells can either activate or inhibit inflammation, microglial phagocytosis, and adult neurogenesis (Baruch et al., 2015; Fisher et al., 2010; Machhi et al., 2021; Monsonego et al., 2003; Spani et al., 2015). In the failed AN1792 ($A\beta_{42}$ peptide) vaccine phase II clinical trial (Orgogozo et al., 2003), the induction of Th1-skewed CD4$^+$ T cells is linked to harmful meningoencephalitis in the brain of some AD patients (Ferrer et al., 2004; Nicoll et al., 2003). Recent reports however indicate that the brain has a higher propensity to recruit CD8$^+$ T cells than CD4$^+$ T cells (Dulken et al., 2019; Smolders et al., 2013). CD8$^+$ T cells infiltrate the brain requiring specificity to cerebral antigens and MHC-I expression in brain endothelial cells (BEC) (Galea et al., 2007). As such, CD8$^+$ T cells are often oligoclonal in the brain neurogenic niches of elderly humans and mice (Dulken et al., 2019) and parenchyma of humans with AD and mice with tauopathy (Chen et al., 2023; Gate et al., 2020; Laurent et al., 2017). CD8$^+$ T cells in the brain resemble activated, tissue resident (CD103$^-$CD69$^+$ and CD103$^+$CD69$^+$), effector memory (T_{EMRA}) cells expressing IFNγ and cytotoxic effector genes (*NKG7* and *GZMA*, *GZMH* and *GZMK*) (Chen et al., 2023; Gate et al., 2020; Laurent et al., 2017; Smolders et al., 2018). IFNγ from CD8$^+$ T cells can cause cognitive decline (Chen et al., 2023; Gate et al., 2020; Laurent et al., 2017) via exacerbating the DAM phenotype in mice with tauopathy (Chen et al., 2023) and inhibiting neural stem cell proliferation in elderly humans and mice (Dulken et al., 2019). However, their role in mouse models of amyloidosis remains debatable, as experiments in mice revealed conflicting results. Depletion of circulating CD8$^+$ T cells in mice with tauopathy (Chen et al., 2023) and genetic loss of T cells and B cells in Rag-2 deficient APP/PS1 mice block neurodegeneration (Spani et al., 2015). On the other hand, in the same APP/PS1 mouse model, the AD-like symptoms (cognitive decline and accumulation of Aβ plaques) are not affected by ablation of CD8$^+$ T cells with antibody (although RNAseq analysis detected alterations in expression of neuronal synapse-related genes) (Unger et al., 2020) nor by the Aβ vaccine-induced increase of Aβ-specific CD8$^+$ T cells in the circulation (Rosset et al., 2015). In 5xFAD mice, CD8$^+$ T cells are reported either not present (Chen et al., 2023) or increased (Su et al., 2023) in the brain. The latter is linked to CXCR6$^+$ CD8$^+$ T cells that protect from AD pathologies (Su et al., 2023), explaining why deficiency in Rag-2 (Marsh et al., 2016), TCRα, or MHC-I or ablation of CXCR6$^+$ PD1$^+$ CD8$^+$ T cells accelerates neuroinflammation in 5xFAD mice (Su et al., 2023).

Here we analyzed CD8$^+$ T cells in the brain of 5xFAD and APP/PS1 mice and postmortem brain tissues from humans with AD and mild cognitive impairment (MCI). We find that manifestation of AD-like symptoms in mice with amyloidosis is mediated by potentially exhausted CXCR6$^+$CD39$^+$CD73$^+$CD8$^+$ T_{RM}-like cells expressing IFNγ and TNFα. Upon infiltration into the brain, CD8$^+$ T cells appear to control function of DAM, as we find these two cells tightly complexed in the hippocampus of mice that develop AD-like pathology and humans with AD, but not in healthy brains. Consistent with the importance of B cells in manifestation of AD-like symptoms (Kim et al., 2021), we now show that they induce the brain-infiltrating CD8$^+$ T cells presumably presenting brain antigens in the periphery. This explains why ablation of B cells or CD8$^+$ T cells decreased CXCR6$^+$CD39$^+$CD73$^+$CD8$^+$ T_{RM}-like cells in the brain and ameliorated AD-like symptoms in 5xFAD mice. Conversely, Aβ vaccine-induced increase of CD8$^+$ T cells in the circulation further enhanced the CXCR6$^+$CD39$^+$CD73$^+$CD8$^+$ T cells and AD-like pathology in the brain.

2. Material and methods

2.1. Animal care and use

The animal protocols were approved by the ACUC institutional review board (ASP 321-LMBI-2022) and performed under the *Guide for the Care and Use of Laboratory Animals* (NIH Publication No. 86-23, 1985). The mice (12–80 weeks of age): C57BL/6J mice (Stock # 000664; Jackson Laboratory, Bar Harbor, ME), APP/PS1 mice (B6.Cg-Tg (APPswe,PSEN1Δ9) 85Dbo/J) (Spani et al., 2015), 5xFAD mice (B6.Cg-Tg;APPSwFILon, PSEN1* M146L* L286V) (Marsh et al., 2016), congenic μMT mice (B6.129S2-*Ighm*^{tm1Cgn}/J;Jackson Laboratory, Bar Harbor, ME), and 5xFAD-BKO mice (created by breeding 5xFAD mice with μMT mice) were maintained in specific pathogen-free environment at the National Institute on Aging (NIA). Transient CD8$^+$ T-cell depletion was performed with intraperitoneal injection of anti-CD8 Ab (200 μg/mouse, clone 2.43, #BE0061, BioXCell) six times for up to 2 months. To induce Aβ-specific CD8$^+$ T cells, mice were i.m. immunized with 3 μg Aβ-CoreS mRNA vaccine encapsulated in LNP once per month for up to 4 times. The vaccine composition is the same as reported elsewhere (Pardi et al., 2015), except it encodes S antigen of HBV (HBsAg, subtype ayw) in-frame fused with the T helper epitope of HBcAg (70–85) and Aβ(1–11) derived from Aβ-CoreS DNA vaccine (Olkhanud et al., 2012).

2.2. Mouse tissues and blood processing

Tissues for immunohistochemistry (IHS) and FACS staining were collected from mice perfused for 15 min with cold PBS after euthanasia with CO_2. One hemisphere of the brain was used for IHS (immune fluorescent, IF) staining and the other one was analyzed by FACS. Single cell suspensions were generated using Adult Brain Dissociation kit for mouse and rat or Multi Tissue Dissociation Kit 1 (MiltenyiBiotec) in GentleMACS™ Dissociator (MiltenyiBiotec, Auburn, CA) following the manufactureŕs instruction. Single cell suspensions of spleen and cervical lymph node (cLN) were prepared using a 70 μm cell strainer (BD Falcon, Bedford, MA) and peripheral blood cells were collected in the tube with 2 mg/ml of Na-heparin (Sigma). Red blood cells were lysed using ACK buffer.

2.3. Flow cytometry (FACS)

Cells were stained with fixable viability dye, pre-incubated with TruStain FcX™ (anti-mouse CD16/32) Antibody (101320, Biolegend), stained with respective fluorophore-conjugated antibodies (listed in Suppl. Table 8), and then fixed with Fixation Buffer (eBioscience). For intracellular cytokine staining, cells were stimulated with 50 ng/ml phorbol 12-myristate 13-acetate (PMA, Tocris Bioscience) and 500 ng/ml ionomycin (Tocris Bioscience) for 1–2 h, then treated with Golgi stop with 10 μM of Monensin (eBioscience) for 3–4 h and intracellular fixation & permeabilization buffer (ThermoFisher, Waltham, MA) following manufacturer's instruction. Antibodies and isotype-matched control antibodies were used at the concentration of 0.2 μg per 10^6 cells. To count FACS cell numbers in FACS, first we determined a total number of viable cells per dissected tissue using Nexcelom Biosciences cell counters (Cellaca MX or Cellometer Vision) after staining with Acridine orange and propidium iodate solution (CS2-0106, Cellometer ViaStain, Nexcelom). Then, equal number of cells per each sample was used for flow cytometry staining and analysis. A total number of cells of interest was calculated using cell counts in each subsequent FACS gating (described in the manuscript, Suppl. SFig. 1A; for example, FSC-SSC, live cell, single cell, CD45$^+$, CD3, and CD8) and the initial number of viable cells. The samples were acquired on FACS Canto II, FACS Symphony A3 (BD) or CytoFLEX (Beckman Coulter, Inc.) and data were analyzed using FlowJo software (Tree Star, Inc.), CytExpert software (Beckman Coulter, Inc.), and Cytobank (https://cytobank.org) respectively. The tSNE CUDA analysis was performed using Cytobank (https://cytobank.org). tSNE

analysis was performed on CD45$^+$ CD3$^+$ cells using total cell sampling from each FCS file with 750 iterations, and a perplexity of 30. Reagents and antibody used are listed in Suppl. Table 8.

2.4. Brain immunohistochemistry/immunofluorescence staining

One brain hemisphere (from PBS perfused mice) was fixed in 4 % PFA/PBS for 24 h and then after washing with PBS, transferred to 30 % sucrose/PBS in 15 ml tubes for 2 days until the brain sank to the bottom. The brain tissues were embedded in OCT compound (4585, Thermo-Fisher), frozen on dry ice, and stored in −80 °C. For cryosection, 30-μm thick coronal sections containing hippocampus were collected with 240 μm interval to obtain eight sets for free-floating IF staining (list of reagents and Abs used is in Suppl. Table 8). In brief, two to six slices of each mouse brain were stained with Abs to β-Amyloid (clone 6E10, cat # 803002) and Iba1 (cat # ab178846) in IF buffer (2 % donkey serum, 2 % BSA, and 0.1 % Triton X-100 in PBS), followed by incubation with fluorophore-conjugated secondary Abs from Abcam (Donkey anti-mouse IgG H&L Alexa Fluor 488/594; Donkey anti-rabbit IgG H&L-Alexa Fluor 568/488). Brain slices were also stained with Abs to CD8a (4SM16, eBioscience™), Collagen IV (ab6586, Abcam), Neurofilament heavy polypeptide (NFH, ab207176, Abcam), and NeuN (ab177487, Abcam), and then with donkey anti-rat IgG H&L-Alexa Fluor 568/647. After DAPI staining, brain sections were mounted with ProLong™ Gold/Diamond Antifade Mountant (Invitrogen) and images were acquired using the Zeiss LSM 710 and 980 confocal microscopes equipped with a × 20/0.8 and a × 20 Plan-Apochromat dry objectives (Carl Zeiss) and analyzed with ImageJ software. For 3-D image reconstruction, IF images were acquired using a confocal laser scanning microscope LSM 880 with Airyscan module (Carl Zeiss AG). The overview of whole section (5.65 mm × 5.65 mm) was captured with 20×/0.5 M27 plan-Apo chromate objective. The CD8$^+$ T cells are considered to be attached to microglia based on their physical contact after magnification with scan zoom x/y: 2/2, total Z-stack of 35 slices with a total of 16 bit depth per area (15–20 of 207.57 μm x 207.57 μm), and processed through ZEN blue software (3.2 edition, Carl Zeiss AG). To confirm, images were processed to construct 3D images using IMARIS software (v. 9.2, Bitplane).

Postmortem human brain tissues, such as formalin-fixed frontal cortex from AD human brains (NCRAD tissue bank, Indianapolis, IN) and brain inferior parietal lobules from humans with non-AD (Braak stage 0–2), MCI (Braak stage 3–5) and AD (Braak stage 5–6) were reported elsewhere (Zhang et al., 2019) (the University of Kentucky Alzheimer's Disease Research Center; Suppl. Table 1, provided by Peisu Zhang, NIA), were embedded with paraffin and sectioned in 4–10 μm with positively charged microscope slides for section collection. For IF staining, brain sections were deparaffined and rehydrated before antigen retrieval with IHC Antigen Retrieval Solution (High pH, 00–4956-58, eBioscience™). IF buffer (5 % donkey serum, 2 % BSA, and 0.1 % Triton X-100 in PBS) was used for blocking, permeabilization and staining with Anti-CD8a Ab (4SM16, eBioscience™), Anti-Collagen IV Ab (ab6586, Abcam), and Ant-Iba1 Ab (ab5076, Abcam). The image acquisition, analysis and construction were performed as above mentioned.

2.5. Bioinformatics analysis

Two publicly available snRNAseq datasets from human brain of patients with AD and healthy controls were analyzed in this study: 1,378,211 single-nucleus transcriptomes from the middle temporal gyrus of 89 individuals from Seattle Alzheimer's Disease Brain Cell Atlas (SEA-AD dataset, https://registry.opendata.aws/allen-sea-ad-atlas) and 70,634 single-nucleus transcriptomes from the prefrontal cortex of 48 individuals (ROSMAP dataset, https://www.nature.com/articles/s41586-019-1195-2). Pre-computed cell type labels were used and only microglial cells were extracted for further analysis. Number of cells per cell type per donor were extracted from full datasets and used as a base for T cell counts normalization. To track changes in T cells proportion T cell counts per patient were normalized by total number of cells per patient (excluding T cells) and by neurons count per patient. The following cell type counts were summed up and denoted as neurons in SEA-AD and ROSMAP datasets correspondingly: L2/3–6 intratelencephalic projecting glutamatergic cortical neuron, vip GABAergic cortical interneuron, pvalb GABAergic cortical interneuron, lamp5 GABAergic cortical interneuron, sst GABAergic cortical interneuron, sncg GABAergic cortical interneuron, near-projecting glutamatergic cortical neuron, corticothalamic-projecting glutamatergic cortical neuron, L6b glutamatergic cortical neuron, chandelier pvalb GABAergic cortical interneuron, caudal ganglionic eminence derived GABAergic cortical interneuron, L5 extratelencephalic projecting glutamatergic cortical neuron; excitatory neurons, inhibitory neurons. Seurat R package was used for processing and bioinformatics analysis of single-cell data [https://doi.org/10.1016/j.cell.2021.04.048].

2.6. Behavioral tests

For the CD8 depletion study, the open field test (OFT) was performed in a circular tub. In brief, the mouse was placed to the center of a circular 140 cm diameter white plastic tub for 15 min and the track was recorded overhead by digital video camera. Activity was quantified by ANY-Maze software (Stoelting; Wood Dale, IL). For spontaneous alternation, mouse was placed in a "cross maze" apparatus containing four red Plexiglas arms radiating at 90° angles. Each arm was 31 cm long and had 21 cm tall walls that sloped outwards such that the width was 4.8 cm wide at the floor and 11.7 cm at the ceiling. Mouse was allowed to freely explore for 15 min while recorded by overhead camera, with activity quantified by ANY-Maze. Alternations were considered to be sequences of three consecutive arm entries to unique arms (e.g., ABC, ABD but not ABA or AAB). Percent alternation was defined as number of alternations divided by number of opportunities for alternation (number of arm entries minus 2). For the Aβ-CoreS vaccine study, the mouse was placed in a 44 x 44 x 30 cm clear Plexiglas arena enclosed inside a dimly lit cubicle for OFT. Activity was detected for 10 min using an array of infrared beams and tracking software (MED-Associates; St Albans, VT). To measure home-cage activity, mouse was singly housed for four days in a digital ventilated caging unit (Tecniplast; Buguggiate, Italy). Each cage was 18 x 36 x 15 cm with transparent walls and sat atop a 4 x 3 grid of capacitive sensors for detecting animal movements (Pernold et al., 2019). While in these cages, all other husbandry was identical to normal housing; i.e., bedding, food, water, nestlet material, room lighting schedule.

2.7. Statistical analysis

All statistical analyses were performed with GraphPad Prism (Prism 10; Graph Pad Software, Inc.). For data with one factor, unpaired *t* test or one-way ANOVA was applied to two or more groups respectively. For data with two factor, two-way ANOVA was carried out. Holm-Šídák post hoc tests were conducted for multiple comparisons. Sample sizes and statistical tests were mentioned in figure legends. The results were presented as the box with whiskers (Min to Max. Show all points) or Mean ± SEM. *P* values computed with GraphPad Prism were shown in figures. Additional information, such as the F statistic, degrees of freedom and *p*-values, are in Supplementary Table 9.

3. Results

3.1. CD8$^+$ T cells increase in the AD brain

Although aging can increase CD8$^+$ T cells in the brain of mice and humans (Dulken et al., 2019), the cells are not found in the brain of 5xFAD mice even at 19-months of age (Chen et al., 2023). To address this discrepancy, first we quantified T cells in the brain of female 3-months and 20-months old C57BL/6 mice of the same background as 5xFAD mice (respectively termed Young and Old; n = 5 mice per group)

using flow cytometer (FACS, gating information in SFig. 1A). Note, all brains used in our study were from saline-perfused mice. Consistent with above-noted report (Dulken et al., 2019), the brain of Old contained significantly higher numbers and frequency of $CD8^+$ T cells than that of Young (SFig. 1B). In contrast, brain $CD4^+$ T cells were only insignificantly increased in Old (SFig. 1B). We also quantified T cells in the brain of male and female 5xFAD and control non-transgenic (WT) littermate mice (8-months and 12–13-months of age; n = 4–11 mice per group). Compared with WT, $CD8^+$ T cells (to markedly lesser extent $CD4^+$ T cells) were significantly increased in the brain (Fig. 1A and SFig. 1C), but not the circulation, of male and female 5xFAD mice at both time points (SFig. 1D). Therefore, unless specified, from here on we mostly experimented with female mice, which exhibit more pronounced AD-like symptoms (Bhattacharya et al., 2014; Poon et al., 2023). In the brain, but not in the circulation, $CD8^+$ T cells predominantly expressed CD11b and markedly upregulated CD103 (Fig. 1B and SFig. 1E, F; gating information in SFig. 1G, H). We also evaluated their inflammatory state using intracellular FACS staining (gating information in SFig. 1I) after *ex vivo* stimulation with PMAi. Compared to WT, the 5xFAD brain $CD8^+$ T cells significantly upregulated expression of TNFα, IFNγ, IL10, and granzyme B (GrB) (Fig. 1C and SFig. 1J), implying that they could be potentially pathogenic. Cryopreserved hippocampi from age-matched 5xFAD and WT mice were also evaluated after IF staining. Consistent with our previous report (Kim et al., 2021), $CD45^{Int}CD11b^+$ microglia cells quantified with FACS positively correlated with IF-stained macrophage-like cells expressing ionized calcium-binding adaptor molecule 1 (Iba1, marker of activated myeloid cells and microglia, SFig. 1K). As in FACS, IF staining detected a marked increase of $CD8^+$ T cells in the parenchyma of hippocampus of 5xFAD compared to WT mice (Fig. 1D and SFig. 1K, L). Notably, significantly higher numbers of $CD8^+$ T cells were tightly complexed with $Iba1^+$ macrophages/microglia around Aβ plaques in 5xFAD than WT mice (Fig. 1D–F and Video 1A,B). We also quantified brain $CD8^+$ T cells in APP/PS1 mice (another model of amyloidosis (Jankowsky et al., 2004)) and TS65dn and DP1Tyb mice (murine Down Syndrome, DS, models that do not generate Aβ plaques in the brain despite three copies of the mouse APP gene and production of elevated amounts of mouse $A\beta_{40}$ and $A\beta_{42}$ (Farrell et al., 2022)). Compared to WT littermates, $CD8^+$ T cells and their $CD11b^+$ and $CD103^+$ subsets were significantly increased in the brain of APP/PS1 (SFig. 1M), but not in DS (SFig. 1N), mice, suggesting that amyloidosis causes $CD8^+$ T cell recruitment into the brain.

To evaluate clinical relevance of our results, we performed IF staining of $CD8^+$ T cells in post-mortem brain tissues from patients with AD (Braak stage VI), mild cognitive impairment (MCI, Braak stage III-V), and healthy elderly people (HC, Braak stage I-II, age/sex-matched, n = 4–6 per group, see Suppl. Table 1) (Zhang et al., 2019). Compared to non-AD, the AD brain parenchyma and perivascular area were significantly increased in $CD8^+$ T cells and their complexes with microglia (Fig. 1G, H, SFig. 2A and Video 2A, B). In MCI brain however there was a trend towards increased $CD8^+$ T cells and their complexes with microglia, but the difference did not reach statistical significance compared with non-AD (Fig. 1G, H). To confirm these results, we analyzed publicly available 1,378,211 and 70,634 single-nucleus transcriptomes from the middle temporal gyrus of 42 AD and 47 non-AD individuals (65–90 years of age, the Seattle Alzheimer's Disease Brain Cell Atlas, SEA-AD, https://registry.opendata.aws/allen-sea-ad-atlas) and the prefrontal cortex of 24 AD and 24 non-AD individuals (74–90 years of age, ROSMAP, https://www.nature.com/articles/s41586-019-1195-2), respectively (Suppl. Table 2, 3). Based on the transcriptional profiles we identified a small cluster of cells with distinct signatures of T cells within dataset of all brain cells (0.08 ± 0.15 % and 0.27 ± 0.040 %) and a subset of immune cells in the brain (1.98 ± 3.54 % and 10.55 ± 11.48 %) in both SEA-AD and ROSMAP datasets, respectively (SFig. 2B, C and Suppl. Table 4, 5). This newly identified brain T cell cluster was dominated by CD8 over CD4 (CD4/CD8 ratio is 1:4.6 or 1:9.7 cells in SEA-AD and ROSMAP datasets, respectively, Fig. 1I, SFig. 2D–G and Suppl. Table 6), which markedly differs from PB that is dominated with $CD4^+$ T cells (CD4/CD8 ratio is at least 1.4) (Amadori et al., 1995). The transcriptional profile of $CD8^+$ T cells indicated that they are non-proliferating (*MKI67*$^-$ and *CCNB1*), effector memory (*CD27*^{Lo}, *CD44*$^+$, *CD69*$^+$, *CD62L/SELL*$^{Lo/-}$, and *IL7R*$^+$), tissue resident (*ITGA1/CD49*$^+$, *ITGAE/CD103*$^+$, and *CXCR6*$^+$) and potentially exhausted (*HAVCR2/Tim-3*^{Hi} and *TIGIT*^{Hi}) memory $CD8^+$ T cells (*CCL5*^{Hi} (Ortiz et al., 1997; Walzer et al., 2003)) with cytolytic functions (*NKG7*$^+$, *GZMA*$^+$, *GZMH*$^+$, *GZMK*$^+$, and *PRF1*$^+$, SFig. 2H and Suppl. Table 7). Normalization to total cell numbers or microglial cells per donor revealed significant increase of $CD8^+$ T cells in the middle temporal gyrus of AD compared to non-AD individuals (SEA-AD cohort, Fig. 1I, J). Presumably because of reduced presence of $CD4^+$ T cells, the Treg cell signature was only detected in a few cells in the large SEA-AD, but not the smaller ROSMAP, dataset (Fig. 1I). Taken together, we concluded that activated $CD8^+$ T cells increase in the brains of mice and humans with AD.

3.2. Brain $CD8^+$ T cells are pathogenic

We hypothesized that the brain $CD8^+$ T cells could be pathogenic in 5xFAD mice, as infection with West Nile virus causes memory impairments by similarly increasing $CD8^+$ T cells and their complex with microglia in the brain (Garber et al., 2019). In 5xFAD mice, $CD8^+$ T cells in the hippocampus indeed positively correlated with hippocampal Aβ plaques and activated microglia/macrophages as well impairments of hippocampus-dependent working memory (Fig. 2A and SFig. 3A). To test the idea, we intraperitoneally (i.p.) treated 8–12-months old 5xFAD mice with anti-CD8 antibody (Ab, depletes circulating $CD8^+$ T cells (Biragyn et al., 2007)) or isotype-matched control Ab for up to two months (respectively, 5xFAD/IgG and 5xFAD/αCD8; n = 10–16 mice per group; Fig. 2B). Although anti-CD8 Ab efficiently ablated $CD8^+$ T cells in the circulation, it only marginally decreased $CD8^+$ T cells in the brain (SFig. 3B, C), presumably due to an inefficient ability of peripherally injected antibody to reach the brain parenchyma (St-Amour et al., 2013) and a relatively long half-life of brain-residing $CD8^+$ T cells. Despite this, anti-CD8 Ab, but not control Ab, significantly decreased numbers of exhausted and tissue resident-like $CD8^+$ T cells ($PD1^+$, $CD103^+$, $CD11b^+$, Fig. 2B) expressing pro- and anti-inflammatory cytokines (Fig. 2C) in the brain of 5xFAD mice to almost the levels in WT mice ($p < 0.05$, 5xFAD/αCD8 compared to 5xFAD/IgG, respectively). While IgG-treated 5xFAD mice exhibited elevated exploration of the center of an open field arena (OFA), suggestive of impaired anxiety response, anti-CD8 Ab treatment normalized this behavior to that of WT mice (5xFAD/aCD8 vs. 5xFAD/IgG mice: $p = 0.048$; 5xFAD/aCD8 vs. WT: $p = 0.509$, Fig. 2D). The total distance travelled did not differ between the groups (SFig. 3D; F2, 35 = 1.294, P=0.2869; WT vs 5xFAD/IgG, P=0.5286; 5xFAD/IgG vs 5xFAD/aCD8, P=0.3174; WT vs 5xFAD/aCD8, P=0.4849), suggesting no motor impairment. Similarly, in the spontaneous alternation test (Jawhar et al., 2012), the impaired working memory of 5xFAD mice ($F_{2,17} = 9.54$, $p < 0.01$; WT vs 5xFAD/IgG $p < 0.01$) was significantly ameliorated by CD8 depletion ($p = 0.039$, 5xFAD/aCD8 vs 5xFAD/IgG, Fig. 2E). Unlike 5xFAD/IgG mice, the behavior of 5xFAD/aCD8 was statistically indistinguishable from WT ($p = 0.127$). Consistent with these results, IF staining revealed that anti-CD8 Ab treatment significantly decreased hippocampal Aβ plaques and $Iba1^+$ microglia in 5xFAD mice ($p < 0.001$ for Aβ plaques and $p < 0.05$ for $Iba1^+$ microglial, compared to 5xFAD/IgG; Fig. 2F, G). We also IF stained the hippocampi for the neurofilament heavy chain isoform (NFH^{SMI35}, a readout for the neuronal/axonal damage in AD) (Brettschneider et al., 2006; Zhan et al., 2015). The increase of NFH aggregates (arrow heads, Fig. 2H) in the subiculum of 5xFAD mice (compared to WT mice, which mostly contained long and thin neurofilaments, arrows in Fig. 2H) was significantly reduced with anti-CD8 Ab treatment ($p = 0.012$ for 5xFAD/αCD8 mice vs 5xFAD/IgG; Fig. 2H, I), indicating amelioration of the neuronal/axonal damage. The NeuN staining (which detects neuronal nuclei) however revealed that

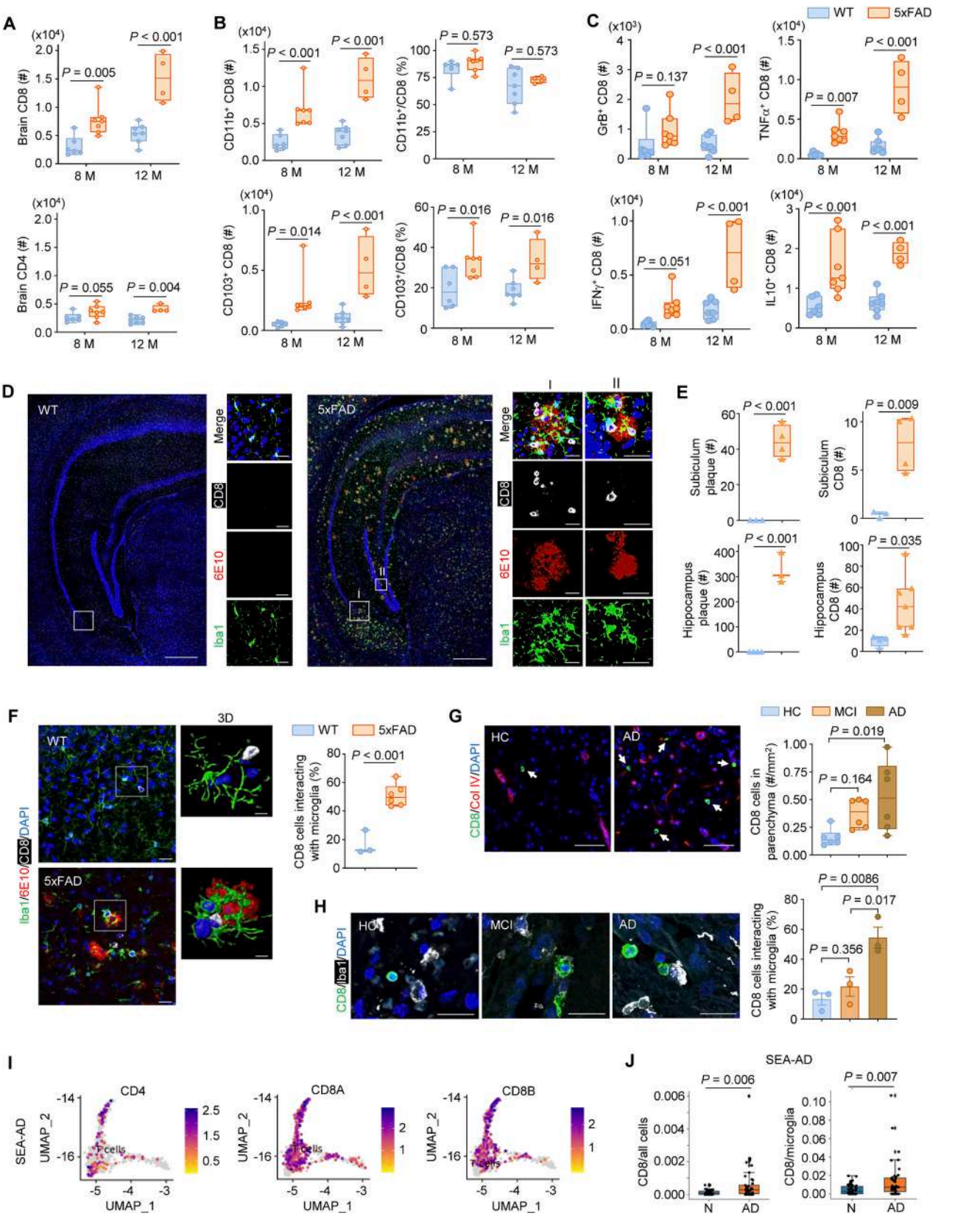

(caption on next page)

Fig. 1. CD8$^+$ T cells increased in the brain of mice and humans. (A) FACS staining results for numbers of CD8$^+$ and CD4$^+$ T cells, (B) numbers (#) and frequency (%) of CD11b$^+$ and CD103$^+$ CD8$^+$ T cells, and (C) numbers of GrB$^+$, TNFα$^+$, IFNγ$^+$ and IL10$^+$ CD8$^+$ cells in the brain of 8 months (8 M) and 12 months (12 M) old WT and 5xFAD female mice. (D) Representative immunofluorescence (IF) staining images and (E) quantification of Aβ plaques (6E10) and CD8$^+$ T cells in the hippocampus and subiculum of female WT and 5xFAD mice. White quadrants in hippocampus sections are for magnified images on the right (D). Scale bars are for 500 μm, whole hippocampus sections, and 20 μm, magnified images for the selected areas. (F) Representative IF images for Iba1/6E10/CD8 staining (left, scale bar is 20 μm). CD8$^+$ T cells are tightly attached to Iba1$^+$ microglia in AD, but not WT, hippocampus (3D reconstruction; scale bar is 5 μm, magnified panels in middle). Right panel is for quantification of CD8$^+$ T cells-Iba1$^+$ microglia complexes (numbers, F). (G and H) Representative IF staining of postmortem human brain tissues from non-AD, MCI and AD people showing the parenchymal presence of CD8$^+$ T cells (G, scale bar is 50 μm) and their complexes with Iba1$^+$ microglia (H, scale bar is 20 μm). Vasculature is stained with anti-collagen IV antibody (Col IV). Right panels are for quantification of CD8$^+$ T cells (G) and their complexes with Iba1$^+$ microglia (H). (I) UMAP plots depict the presence of CD4$^+$, CD8A$^+$ and CD8B$^+$ T cells in SEA-AD datasets. (J) Normalization of CD8$^+$ T cells in AD individuals in SEA-AD cohort. Each dot in A-C and E-H is for independent sample. n = 4–7 mice per group in A-C; n = 3–7 mice per group in E; n = 3–6 mice per group in F; n = 6 brains per group in G; n = 3 brains per group in H. * P<0.05, ** P<0.01, *** P<0.001; Two-way ANOVA tests were performed for A-C, unpaired t-tests were performed for E, F and J, one-way ANOVA tests were performed for G and H. Holm-Šídák post hoc tests were used for multiple comparisons, and p-values were shown as noted.

compared to WT, both 5xFAD/αCD8 and 5xFAD/IgG mice were comparably decreased in NeuN$^+$ neurons (SFig. 3E), suggesting that the CD8$^+$ T cell ablation does not restore the neuronal loss. Hence, progression of the AD-like pathology can be blocked by depleting peripheral CD8$^+$ T cells that infiltrate into the brain.

3.3. Peripherally activated CD8$^+$ T cells enhance the AD pathology in the brain

Since leakage of Aβ peptides into the circulation (Da Mesquita et al., 2018) may induce Aβ-specific T cells, we wondered whether Aβ vaccine would further enhance these CD8$^+$ T cells and thus, the AD-like pathology. 5xFAD mice (2–3 months old, early onset of AD) were injected with Aβ-CoreS RNA vaccine, which expresses human Aβ$_{1\text{-}11}$ fused to HBsAg (Olkhanud et al., 2012), or control RNA LNP carrier (once per month four times, 5xFAD/Aβ-CoreS and 5xFAD/LNP, respectively, n = 8–10 mice per group, Fig. 3A). The Aβ$_{1\text{-}9}$ region appeared to encode a naturally processed MHC-I (H2-Kb) epitope (https://tools.iedb.org/mhcnp). Then, brains were analyzed for CD8$^+$ T cells with FACS and hippocampi were IF stained to quantify CD8$^+$ T cells and the neurofilament heavy chain isoform (NFH^{SMI35}, a read out for the neuronal/axonal damage in AD) (Brettschneider et al., 2006; Zhan et al., 2015). Compared with 5xFAD/LNP mice, 5xFAD/Aβ-CoreS significantly increased CD8$^+$ T cells in the brain, particularly in the dentate gyrus and subiculum of the hippocampus ($p < 0.05$, Fig. 3B, C). These CD8$^+$ T cells upregulated expression of exhaustion markers (PD1$^+$ and Lag3$^+$) and pro- and anti-inflammatory cytokines (TNFα$^+$, IFNγ$^+$, IL-10$^+$, TGFβ$^+$, and GrB$^+$, $p < 0.01$ compared with 5xFAD/LNP, Fig. 3D,E and SFig. 4A, B). Notably, the subiculum in 5xFAD/Aβ-CoreS significantly increased NFH aggregates compared to 5xFAD/LNP mice (Fig. 3F), supporting the idea that CD8$^+$ T cells contribute to neuronal dysfunction (Unger et al., 2020). We then repeated the experiment in 7–8 months old 5xFAD mice (n = 8–10 mice per group, Fig. 3G), at the age when the AD symptoms fully manifest (Kim et al., 2021). Compared with 5xFAD/LNP, the Aβ-CoreS immunization only marginally exacerbated behavioral impairments of 5xFAD mice, such as open field exploration and nocturnal homecage activity (SFig. 4C, D). Despite this, compared to 5xFAD/LNP mice, subiculum of 5xFAD/Aβ-CoreS mice contained significantly higher numbers of Aβ plaques and CD8$^+$ T cells (Fig. 3G–I and SFig. 4E). As in the younger mice (Fig. 3D, E), the immunization further upregulated CD8$^+$ T cells with exhausted and tissue residence phenotype (Fig. 3J and SFig. 4F). Control LNP immunization did not increase numbers nor affect phenotype of CD8$^+$ T cells in the brain of 5xFAD mice (SFig. 4G). Also, presumably due to absence of MHC-II epitope in Aβ-CoreS (Olkhanud et al., 2012), immunization did not increase brain CD4$^+$ T cells (SFig. 4H). Hence, upon peripheral activation, the brain antigen (Aβ)-specific CD8$^+$ T cells can infiltrate and upregulate the AD-like pathology (NFH aggregates and Aβ plaques) in the brain. However, this increase appeared to require expression of the antigen in the brain, as Aβ-CoreS immunization did not affect CD8$^+$ T cells and Iba1$^+$ microglia in the hippocampus of non-transgenic WT mice (IF staining, n = 3–4 female 11 month-old mice per group; SFig. 4I,J).

3.4. The AD upregulates unique CD8$^+$ T cells requiring B cells

We previously reported that genetic or antibody-mediated loss of B cells blocks manifestation of AD in 5xFAD, APP/PS1, and 3xTgAD mice (Kim et al., 2021). Because these B cells phenotypically resemble 4-1BBL$^+$ B cells that induce GrB$^+$CD8$^+$ T cells in aging (Lee-Chang et al., 2014; Lee-Chang et al., 2016), we wondered whether B cells promote AD via inducing and increasing brain CD8$^+$ T cells. Consistent with this idea, a retroactive analysis of 5xFAD mice, where AD does not progress due to depletion of B cells with anti-CD20/B220 Ab (Kim et al., 2021), detected a marked decrease of exhausted-like CD8$^+$ T cells in the brain (SFig. 5A). To confirm this, we quantified CD8$^+$ T cells in the brain and cLN of WT mice and age-matched 5xFAD mice that are sufficient or deficient in B cells (5xFAD and 5xFAD-BKO, respectively). As noted above, compared to WT mice, CD8$^+$ T cells were significantly increased in the brain, but not cLN, of 5xFAD mice (in terms of numbers and frequency, Fig. 4A,B and SFig. 5B–D). This increase, particularly pro-inflammatory and cytolytic CD8$^+$ T cell subsets, was completely reversed in 5xFAD-BKO mice ($p < 0.05$, both females and males) to almost the levels of WT mice (Fig. 4A, B and SFig. 5C, D). Using the t-distributed stochastic neighbor embedding (tSNE) analysis after FACS staining, we found a unique cluster of brain CD8$^+$ T cells that is enriched in 5xFAD mice (from hereon, termed DP8, marked with circles in Fig. 4C). It expressed high levels of markers of tissue residence and exhaustion (CD103, CD11b, PD-1, Lag-3, and Tim-3) and ectonucleotidases CD39 and CD73 (Fig. 4C). Compared with WT mice, the DP8 cells were significantly increased in the brain of male and female 5xFAD mice (Fig. 4D, E) and APP/PS1 mice (SFig. 5E). Resembling recently reported protective CD8$^+$ T cells in AD (Su et al., 2023), most of them expressed CXCR6 (SFig. 5F). The CXCR6 expression alone or with CD39 and CD73 appeared to be a feature of the brain CD8$^+$ T cells. In contrast, cLN mostly contained CD39$^-$CD73$^+$ (to a lesser extent CD39$^-$CD73$^-$) CD8$^+$ T cells (SFig. 5F). Notably, the brain DP8 cell increase was almost completely lost in 5xFAD-KO mice (Fig. 4C–F), which are protected from AD-like pathology (Kim et al., 2021). Conversely, the Aβ-CoreS immunization significantly increased DP8 cells in the brain (Fig. 4G and SFig. 5G, and also Fig. 3B–E) and upregulated AD-like symptoms (Fig. 3F, H). Control WT mice did not increase these cells nor activated microglia in the brain after Aβ-CoreS immunization (SFig. 54J). Taken together, we concluded that amyloidosis exacerbates AD-like pathology by increasing pathogenic brain CD8$^+$ T cells, including DP8 cells, at least in part via B cells.

4. Discussion

During preparation of this manuscript, Su et al. reported that 5xFAD mice with amyloidosis increase brain CXCR6$^+$ CD8$^+$ T cells to protect from AD pathology (Su et al., 2023). Our results also indicate that 5xFAD mice increase CXCR6$^+$ CD8$^+$ T cells in the brain, but it is to exacerbate AD-like pathology as in recently reported mice with tauopathy (Chen et al., 2023). Considering that CXCR6 is expressed on most brain CD8$^+$ T cells, it probably will not discriminate protective (Su et al., 2023) and

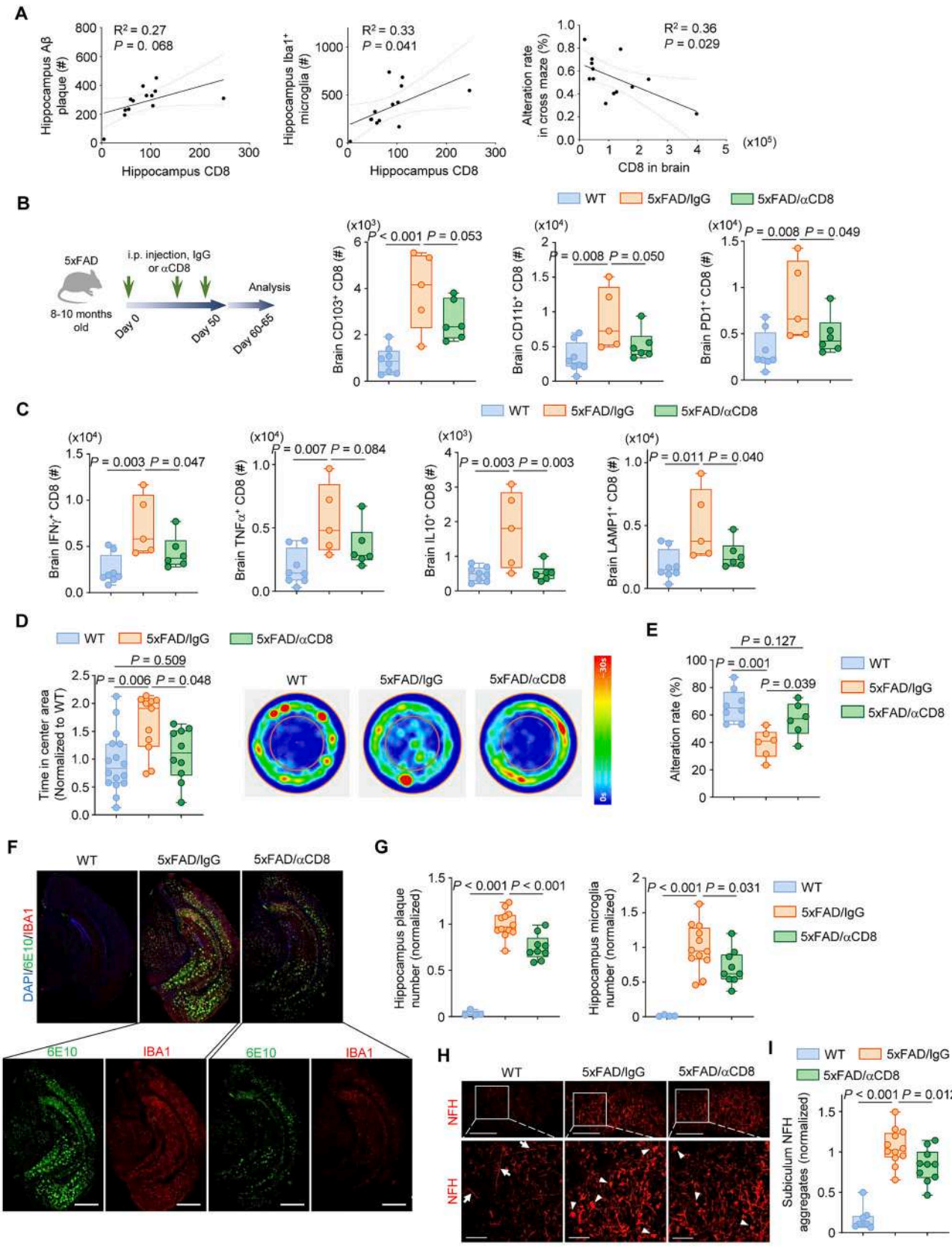

(caption on next page)

Fig. 2. Depletion of CD8$^+$ T cells reverses AD-like pathology in 5xFAD mice. (A) Correlations between CD8$^+$ T cell and numbers of Aβ plaque (i), or Iba1$^+$ microglia (ii) in the hippocampus after IF staining; and FACS quantified brain CD8$^+$ T cell counts and behavioral impairment in cross maze (iii) of WT and 5xFAD mice (10–13 months old female mice). (B-I) Shown are schema (B) and results of the CD8$^+$ T cells depletion experiment, including brain CD8$^+$ T cell subsets (numbers quantified with FACS, B and C); and open field test (D) and continuous spontaneous alternation rate in cross maze (E). WT and 5xFAD mice (8–10 months old females) were treated with anti-CD8 (αCD8) and control antibody (IgG). In D, left panel is quantification of time spent in the center area of open field (normalized to WT group); right panel is for representative heatmaps for the time spent in open field (center area shown as red circle). (F-I) Shown are representative IF staining images and quantification of Aβ plaques and Iba1$^+$ microglia in the hippocampus (F and G) and neurofilament heavy chain (NFH, normalized to 5xFAD/IgG group) in subiculum (H, I). Scale bar is 1 mm (F) and 200 μm (upper panel, H) and 50 μm (lower magnified images, H). Arrows and arrowheads in H indicate long neurofilaments and NFH aggregates, respectively. Dots are for independent mice in A-E, G and I, n = 13 mice in A; n = 5–8 mice per group in B-C; n = 10–16 mice per group in D; n = 6–8 mice per group in E; n = 4–12 mice per group in G; n = 8–12 mice per group in I. D, G and I are from 2 independent experiments. Linear regressions were computed for A, one-way ANOVA tests were performed for B-E, G and I. Holm-Šídák post hoc tests were used for multiple comparisons, and *p*-values were shown as noted.

pathogenic CD8$^+$ cells. The two subsets may also be present within brain CD8$^+$ cells, which we and others find increased in humans with MCI, AD, and tauopathy (Chen et al., 2023; Laurent et al., 2017; Smolders et al., 2018; Yousef et al., 2019). By analyzing CD8$^+$ T cells in the brain of mice that ameliorated AD symptoms because of the genetic or antibody-mediated ablation of B cells (Kim et al., 2021) or treatment with anti-CXCL16 or anti-CD8 Ab), we narrowed the AD-promoting cells to a cluster of CD39$^+$ and possibly CD73$^+$ CD8$^+$ T_{RM}-like (DP8) cells expressing exhaustion markers and proinflammatory cytokines IFNγ and TNFα. Treatment with anti-CD8 Ab or B-cell deficiency ablates DP8 cells in the brain and reverses the AD-like pathology, including accumulation of Aβ plaques and NFH aggregates. Conversely, immunization with Aβ vaccine upregulates DP8 cells and exacerbates the AD-like pathology in 5xFAD mice. The remaining brain CD8$^+$ T cells, which are not affected by these manipulations, presumably contain the AD-protecting subsets. Since both protective and pathogenic CD8$^+$ T cell subsets will be ablated in MHC-I deficient (KO) 5xFAD mice, we can only speculate that the exacerbation of AD pathology reported in these mice (Su et al., 2023) could be due to inflammation or/and activation of other immune cells that cytolytic/pro-inflammatory CD8$^+$ T cells control (Li et al., 2022). Moreover, MHC-I molecules are also implicated in non-immunological functions in the brain. It is upregulated in AD microglia to utilize in developmental synapse elimination and Tau pathology (Kellogg et al., 2023); and its β2m deficiency increases glutamatergic and GABAergic synapse density in the brain (Glynn et al., 2011). MHC-I molecules can activate or inhibit cell signaling via binding ITAM or ITIM (immunoreceptor tyrosine-based activation or inhibitory motif)-containing receptors, including leukocyte immunoglobulin-like receptor and C-lectin-like receptors (Borges et al., 1997; Getahun and Cambier, 2015).

Our results suggest that the deposition of Aβ plaques alone is sufficient to induce infiltration of CD8$^+$ T cells into the brain in 5xFAD and APP/PS1 mice. The Aβ plaque-induced brain inflammation upregulates CXCL16, which will then recruit CXCR6$^+$ CD8$^+$ T cells (Castillo et al., 2017; Piehl et al., 2022). This presumably explains why we did not detect increase of CD8$^+$ T cells in the brain of TS65dn and DP1Tyb mice, which do not generate Aβ plaques (despite production of elevated amounts of $Aβ_{40}$ and $Aβ_{42}$) (Farrell et al., 2022). Since the recruitment of CD8$^+$ T cells in the brain parenchyma requires antigen specificity and expression of MHC-I machinery in BEC (Yousef et al., 2019), we think that the brain-infiltrating CD8$^+$ T cells are induced by Aβ (and other aberrantly upregulated cerebral antigens) in the periphery, possibly in the deep cLN (Schupf et al., 2008). Although the mechanism of their induction is a topic of a different study, the present study implicates B cells. First, B cells in AD resemble 4BL-like cells of elderly mice and humans (Kim et al., 2021), which induce antigen-specific cytolytic CD8$^+$ T cells (Lee-Chang et al., 2014; Lee-Chang et al., 2016). Second, the loss of B cells (either via genetic or antibody-mediated ablation with anti-CD20 Ab treatment) not only blocks progression of AD symptoms (Kim et al., 2021), but also decreases DP8 cells in the brain of AD mice. Consistent with importance of B cells in exacerbation of the DAM phenotype and thus AD-like pathology (Kim et al., 2021), we think that B cells use CD8$^+$ T cells to upregulate activity (i.e. inflammation) of microglia, thereby promoting neurodegeneration (Meda et al., 1995). We find CD8$^+$ T cells are tightly attached to activated microglia around Aβ plaques in the brain of 5xFAD mice and humans with AD, but not in non-AD mice and humans. Our preliminary results suggest that this complex does not affect viability of ex vivo cultured microglia from 5xFAD mice during at least 48 h of contiguous attachment of brain CD8$^+$ T cells. We think that the brain CD8$^+$ T cells increase Aβ plaques and thus, AD-like pathology by affecting the DAM phenotype and phagocytosis. Similar CD8$^+$ T cell-microglia complexes are linked to cognitive decline in aging and after infection with neurotropic viruses, where IFNγ from CD8$^+$ T cells activates microglia to cause synaptic elimination and neuronal apoptosis (Ekdahl et al., 2003; Garber et al., 2019; van Dyck et al., 2023). This explains why the immunization with Aβ vaccine increases DP8 cells in the brain and upregulates brain Aβ plaques and NFH aggregates and conversely, the loss of B cells in AD mice reduces brain IFNγ$^+$ and TNFα$^+$ DP8 cells and decreases the DAM phenotype while increasing homeostatic TGFβ$^+$ microglia (Kim et al., 2021). In addition to IFNγ and TNFα, 5xFAD mouse brain DP8 cells significantly upregulate expression of cytolytic enzyme GrB as well immunoregulatory molecules, such as IL-10, TGFβ, CD39, and CD73. Thus, considering upregulation of the MHC-I machinery in inflamed or aged brain (Smith et al., 2015; VanGuilder Starkey et al., 2012; Yousef et al., 2019) and association of MHC-I gene polymorphism with late onset of AD (Guerini et al., 2009), it is also possible that brain CD8 cells elicit an MHC-I-dependent cytolytic activity on neurons or other brain cells as in killing of catecholaminergic neurons (Cebrian et al., 2014). The upregulation of MHC-I in BEC (Yousef et al., 2019) may also lead to CD8$^+$ T cell-mediated intracerebral hemorrhage in people with cerebral amyloid angiopathy and possibly after active immunization with Aβ-vaccine. The DP8 cells may also use IL-10 to alternatively activate microglia and inhibit neurogenesis (Sanchez-Molina et al., 2022), or ectoenzymes CD39 and CD73 to affect neuronal plasticity or function of microglia and astrocytes by hydrolyzing extracellular ATP to adenosine (Garcia-Gil et al., 2021). Bioinformatics analysis of publicly available two independent databases (ROSMAP and SEA-AD) for human brain single nuclear RNA sequencing suggests at least some of these pathways could be involved in humans. Human AD brain appears to accumulate CXCR6$^+$ $CD8^{\pm}_{EMRA}$-like (CD27^{Lo}, CD44$^+$, CD69$^+$, CD62L/SELL$^{Lo/}$, and IL7R^{High}) expressing markers of tissue residence (CD49a/ITGA1$^+$, and CD103/ITGAE$^+$), exhaustion (HAVCR2$^+$,and Lag-3$^+$), and inflammation/cytotoxicity (CCL5^{Hi}, NKG7$^+$, GZMA$^+$, GZMH$^+$, GZMK$^+$), resembling our DP8 cells and the brain CD8$^+$ T cells in tauopathy and aging (Chen et al., 2023; Laurent et al., 2017; Smolders et al., 2018; Yousef et al., 2019). Future functional studies will reveal the importance of any of these pathways in promoting cognitive decline in AD.

Taken together, we demonstrate that manifestation of AD-like pathology in mice with amyloidosis and possibly in humans with AD is mediated by CXCR6$^+$ CD8$^+$ T cells, including IFNγ$^+$ CD39$^+$CD73$^+$CD8$^+$ T_{RM}-like cells. We show that upon peripheral induction with aberrantly produced cerebral antigens (Aβ), CD8$^+$ T cells infiltrate the brain parenchyma and exacerbate AD-like pathology. Considering the presence of clonally expanded (i.e. antigen-specific) CD8$^+$ T_{EMRA} in the CSF and PBMCs of patients with AD (Gate et al., 2020), our results caution against the active immunization with cerebral antigens (Aβ or Tau) to generate beneficial antibody, as it may also boost harmful CD8$^+$ T cells. This probably explains why the Aβ peptide vaccine is linked to

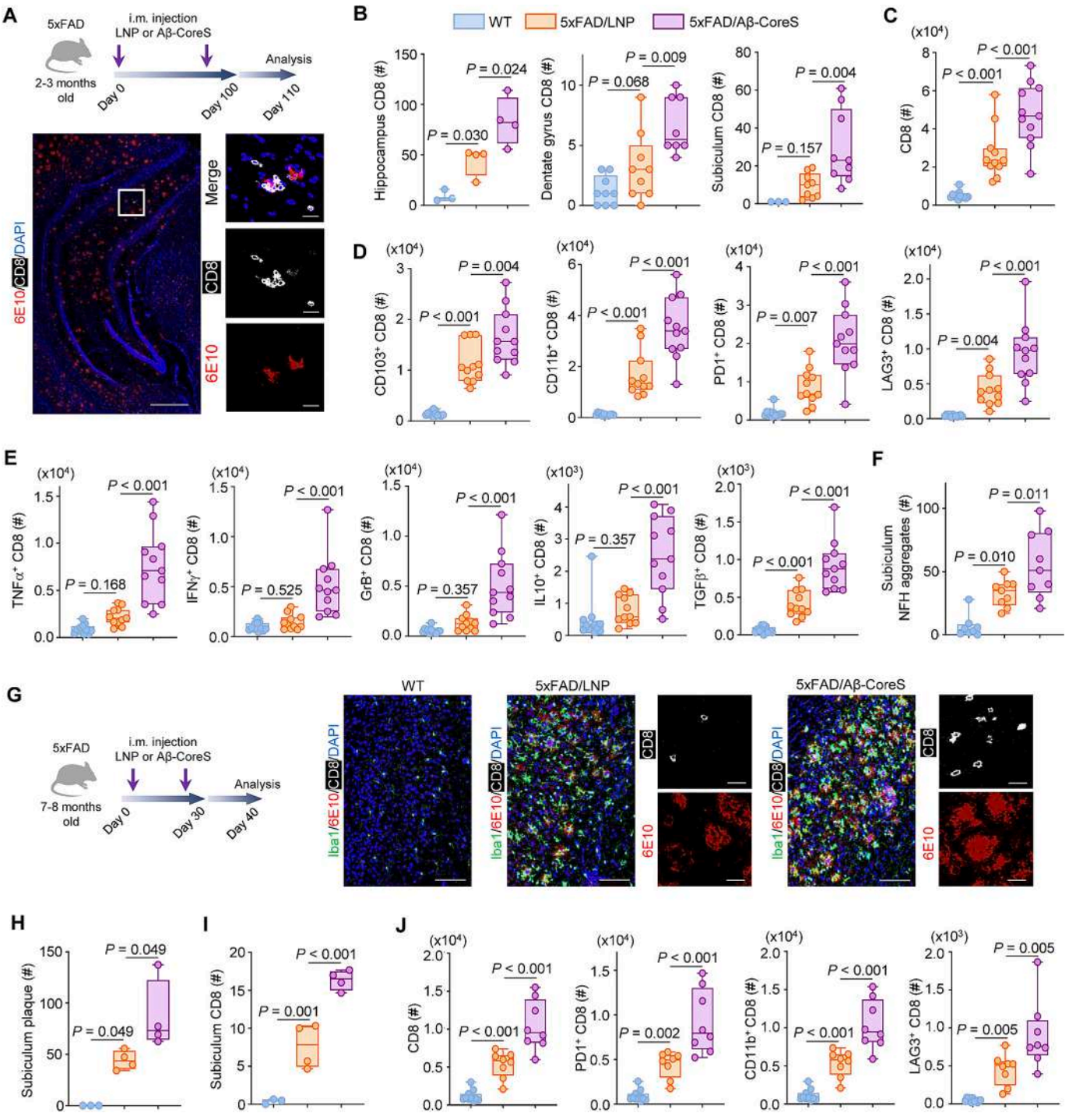

Fig. 3. Aβ-vaccine increases brain CD8$^+$ T cells to exacerbate AD. Female 2–3 months (A-F) and 7–8 months (G-J) old 5xFAD mice were i.m. immunized with Aβ-CoreS/LNP vaccine and control LNP. Shown are representative IF image of hippocampus stained with anti-CD8 and 6E10 Abs (A, scale bar is 500 μm in whole hippocampus image and 20 μm in magnified images, white square) and numbers of CD8$^+$ T cells in hippocampus, dentate gyrus, and subiculum (IF staining, B), activated/exhausted CD8$^+$ T cells in the brain (FACS results, C-E), and NFH aggregates in the subiculum (IF staining, F). Representative IF staining images of the subiculum of WT and 5xFAD mice immunized with Aβ-CoreS or control LNP are shown in G (left panels, scale bar 100 μm, and its magnified area, right panels, scale 20 μm) and respective quantification of Aβ plaques (H) and CD8$^+$ T cells in the subiculum (I). Activated brain CD8$^+$ T cells were quantified with FACS (J). Dots in B-F and H-J are for independent mice. n = 3–4 mice per group for hippocampus quantification and n = 8–9 brain slices from 3 mice per group for dentate gyrus and subiculum quantification in B, C and F; n = 11–12 mouse brains per group in D and E; n = 3–4 mice per group in H-I; n = 8–11 mice per group in J. One-way ANOVA tests were performed for B-F, H-J. Holm-Šídák post hoc tests were used for multiple comparisons, and *p*-values were shown as noted.

meningoencephalitis in some AD patients in an AN1792 phase II clinical vaccine trial (Orgogozo et al., 2003). We instead propose that strategies that inactivate B cells or CD8$^+$ T cells could be a safer and efficient alternative to delay the progression of AD.

CRediT authorship contribution statement

Xin Wang: Methodology, Investigation, Formal analysis. **Britney Campbell:** Investigation. **Monica Bodogai:** Investigation, Formal

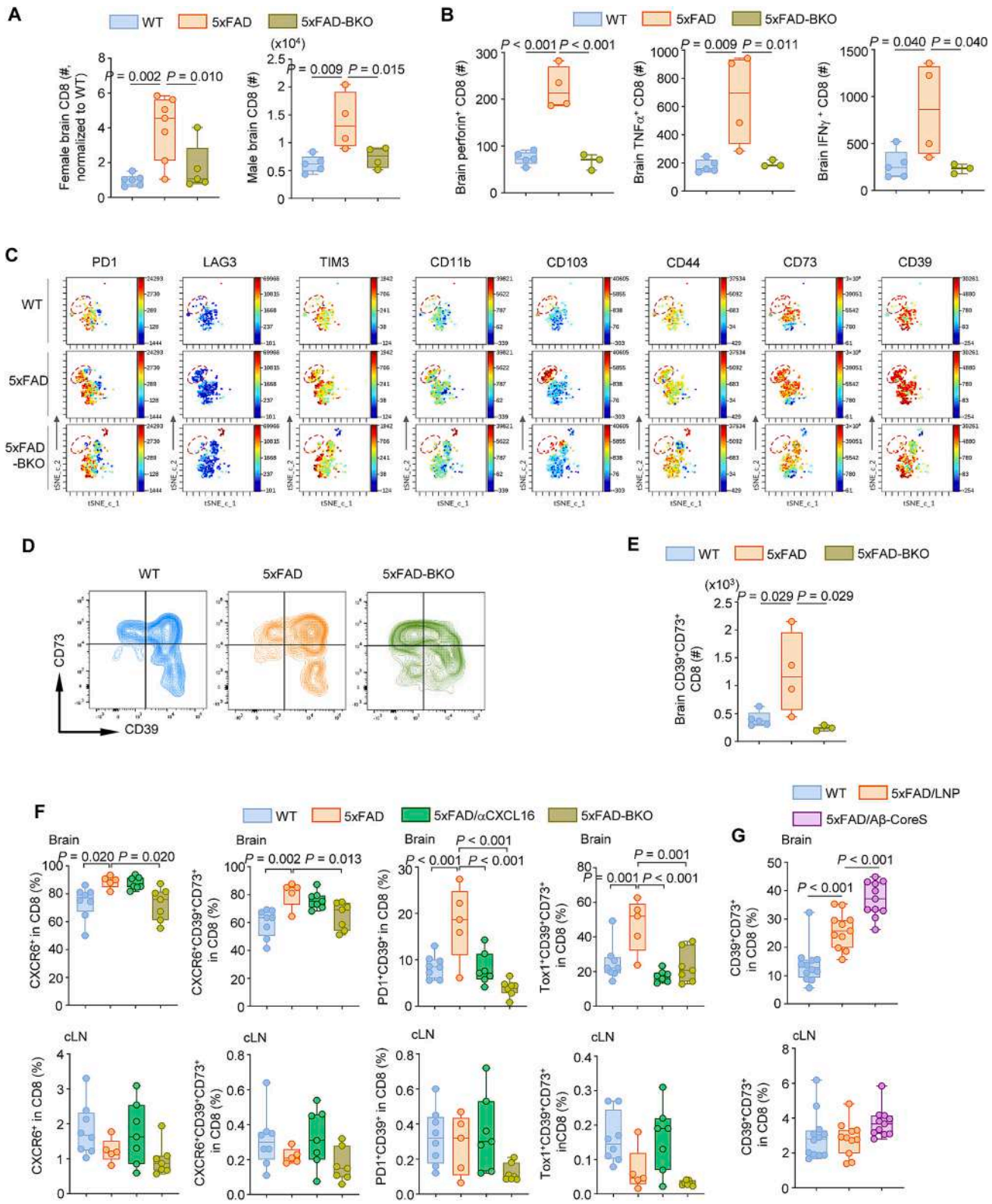

Fig. 4. B cells induce brain-infiltrating $CD8^+$ T cells in 5xFAD mice. In 5xFAD-BKO mice, the increase of activated $CD8^+$ T cells (A) and their activated subsets (B) in the brain of female and male 5xFAD is reversed to the levels of WT mice. Shown are numbers of cells quantified by FACS. tSNE plot showing enrichment of PD1, LAG3, TIM3, CD11b, CD103, CD44, CD73 and CD39-expressing T cells in the brain from 5xFAD mice as compared to 5xFAD-BKO and WT mice as detected by FACS (Red circle, C). FACS dot plots (D) and quantification (E) of $CD39^+CD73^+$ $CD8^+$ T cells in the brain of female WT, 5xFAD, and 5xFAD-BKO mice. (F) The percentage of CXCR6 alone or with $CD39^+CD73^+$ and $PD1^+$ or $Tox1^+$ in $CD8^+$ T cells in the brain and cLN of 5xFAD mice with CXCL16 depleted or BKO. (G) $CD39^+CD73^+$ $CD8^+$ T cells in the brain and cLN of 5xFAD mice immunized with Aβ-CoreS as in Fig. 3G. n = 5–7 female mice and 4–5 male mice per group in A; n = 3–5 mice per group in B and E; n = 5–8 mice per group in F; n = 11–12 mice per group in G; One-way ANOVA tests were performed for B-F, H-J. Holm-Šídák post hoc tests were used for multiple comparisons, and *p*-values were shown as noted.

analysis, Data curation. **Ross A. McDevitt:** Investigation, Formal analysis, Data curation. **Anton Patrikeev:** Formal analysis, Data curation. **Fedor Gusev:** Data curation. **Emeline Ragonnaud:** Investigation, Formal analysis. **Konda Kumaraswami:** Methodology. **Sophie Shirenova:** Investigation. **Karin Vardy:** Investigation. **Mohamed-Gabriel Alameh:** Methodology. **Drew Weissman:** Methodology. **Hellen Ishikawa-Ankerhold:** Investigation. **Eitan Okun:** Investigation. **Evgeny Rogaev:** Investigation. **Arya Biragyn:** Writing – review & editing, Writing – original draft, Supervision, Project administration, Investigation, Conceptualization.

Declaration of competing interest

The authors declare that they have no known competing financial interests or personal relationships that could have appeared to influence the work reported in this paper.

Data availability

Data will be made available on request.

Acknowledgments

We are grateful to Quia Claybourne (NIA/NIH) for technical support, Peisu Zhang (NIA/NIH) and Kelley Farber (the National Centralized Repository for Alzheimer's Disease and Related Dementias, NCRAD, Indianapolis, IN) for providing brain tissues from postmortem humans with and without AD. Samples from NCRAD, which receives government support under a cooperative agreement grant (U24 AG021886) awarded by the National Institute on Aging (NIA), were used in this study. We thank contributors who collected samples used in this study, as well as patients and their families, whose help and participation made this work possible. We thank the SFB 914 project Z01-Germany (Dr. Hellen Ishikawa-Ankerhold) to support with the microscope images. The snRNA-seq results published here are in part based on data obtained from the AD Knowledge Portal (https://adknowledgeportal.org). ROSMAP snRNA-seq data were generated from postmortem brain tissue provided by the Religious Orders Study and Rush Memory and Aging Project (ROSMAP) cohort at Rush Alzheimer's Disease Center, Rush University Medical Center, Chicago, under NIH grants U01AG061356 (De Jager/Bennett), RF1AG057473 (De Jager/Bennett), and U01AG046152 (De Jager/Bennett) as part of the AMP-AD consortium, as well as NIH grants R01AG066831 (Menon) and U01AG072572 (De Jager/St George-Hyslop).

CRediT authorship contribution statement

Xin Wang: performed experiments, collected and analyzed data, writing and editing, and methodology. Britney Campbell, Monica Bodogai, Ross McDavid, Emeline Ragonnaud, Konda Kumaraswami, Karin Vardy, and Sophie Shirenova: performed experiments, collected and analyzed data, and methodology. Anton Patrikeev and Fedor Gusev provided bioinformatics support. Mohamed-Gabriel Alameh and Drew Weissman provided essential reagent (RNA vaccine). Hellen Ishikawa-Ankerhold, Evgeny Rogaev, and Eitan Okun curated and supervised and provided critical interpretation. Arya Biragyn conceived, designed, and supervised the study and wrote the manuscript.

Funding

This research was supported by the Intramural Research Program of the National Institute on Aging, NIH.

Data and materials availability

All data associated with this study can be found in the paper or supplementary materials.

Appendix A. Supplementary data

Supplementary data to this article can be found online at https://doi.org/10.1016/j.bbi.2024.08.045.

References

Amadori, A., et al., 1995. Genetic control of the CD4/CD8 T-cell ratio in humans. Nat. Med. 1, 1279–1283.
Baik, S.H., et al., 2014. Migration of neutrophils targeting amyloid plaques in Alzheimer's disease mouse model. Neurobiol. Aging 35, 1286–1292.
Baruch, K., et al., 2015. Breaking immune tolerance by targeting Foxp3(+) regulatory T cells mitigates Alzheimer's disease pathology. Nat. Commun. 6.
Bhattacharya, S., et al., 2014. Galantamine slows down plaque formation and behavioral decline in the 5XFAD mouse model of Alzheimer's disease. PLoS One 9, e89454.
Biragyn, A., et al., 2007. Tumor-associated embryonic antigen-expressing vaccines that target CCR6 elicit potent CD8+ T cell-mediated protective and therapeutic antitumor immunity. J. Immunol. 179, 1381–1388.
Bombois, S., et al., 2007. Absence of beta-amyloid deposits after immunization in Alzheimer disease with Lewy body dementia. Arch. Neurol. 64, 583–587.
Borges, L., et al., 1997. A family of human lymphoid and myeloid Ig-like receptors, some of which bind to MHC class I molecules. J. Immunol. 159, 5192–5196.
Brettschneider, J., et al., 2006. The neurofilament heavy chain (NfH) in the cerebrospinal fluid diagnosis of Alzheimer's disease. Dement. Geriatr. Cogn. Disord. 21, 291–295.
Castillo, E., et al., 2017. Comparative profiling of cortical gene expression in Alzheimer's disease patients and mouse models demonstrates a link between amyloidosis and neuroinflammation. Sci. Rep. 7, 17762.
Cebrian, C., et al., 2014. MHC-I expression renders catecholaminergic neurons susceptible to T-cell-mediated degeneration. Nat. Commun. 5, 3633.
Chen, X., et al., 2023. Microglia-mediated T cell infiltration drives neurodegeneration in tauopathy. Nature 615, 668–677.
Da Mesquita, S., et al., 2018. Functional aspects of meningeal lymphatics in ageing and Alzheimer's disease. Nature 560, 185–191.
Dulken, B.W., et al., 2019. Single-cell analysis reveals T cell infiltration in old neurogenic niches. Nature 571, 205–210.
Ekdahl, C.T., et al., 2003. Inflammation is detrimental for neurogenesis in adult brain. PNAS 100, 13632–13637.
Farrell, C., Mumford, P., Wiseman, F.K., 2022. Rodent Modeling of Alzheimer's Disease in Down Syndrome: In vivo and ex vivo Approaches. Front. Neurosci. 16, 909669.
Ferrer, I., et al., 2004. Neuropathology and pathogenesis of encephalitis following amyloid-beta immunization in Alzheimer's disease. Brain Pathol. 14, 11–20.
Fisher, Y., et al., 2010. T cells specifically targeted to amyloid plaques enhance plaque clearance in a mouse model of Alzheimer's disease. PLoS One 5, e10830.
Galea, I., et al., 2007. An antigen-specific pathway for CD8 T cells across the blood-brain barrier. J. Exp. Med. 204, 2023–2030.
Garber, C., et al., 2019. T cells promote microglia-mediated synaptic elimination and cognitive dysfunction during recovery from neuropathogenic flaviviruses. Nat. Neurosci. 22, 1276–1288.
Garcia-Gil, M., et al., 2021. Metabolic Aspects of Adenosine Functions in the Brain. Front. Pharmacol. 12, 672182.
Gate, D., et al., 2020. Clonally expanded CD8 T cells patrol the cerebrospinal fluid in Alzheimer's disease. Nature 577, 399–404.
Getahun, A., Cambier, J.C., 2015. Of ITIMs, ITAMs, and ITAMis: revisiting immunoglobulin Fc receptor signaling. Immunol. Rev. 268, 66–73.
Glenner, G.G., Wong, C.W., 1984. Alzheimer's disease: initial report of the purification and characterization of a novel cerebrovascular amyloid protein. Biochem. Biophys. Res. Commun. 120, 885–890.
Glynn, M.W., et al., 2011. MHCI negatively regulates synapse density during the establishment of cortical connections. Nat. Neurosci. 14, 442–451.
Gotz, J., Bodea, L.G., Goedert, M., 2018. Rodent models for Alzheimer disease. Nat. Rev. Neurosci. 19, 583–598.
Goverman, J., 2009. Autoimmune T cell responses in the central nervous system. Nat. Rev. Immunol. 9, 393–407.
Guerini, F.R., et al., 2009. HLA-A*01 is associated with late onset of Alzheimer's disease in Italian patients. Int. J. Immunopathol. Pharmacol. 22, 991–999.
Jankowsky, J.L., et al., 2004. Mutant presenilins specifically elevate the levels of the 42 residue beta-amyloid peptide in vivo: evidence for augmentation of a 42-specific gamma secretase. Hum. Mol. Genet. 13, 159–170.
Jawhar, S., et al., 2012. Motor deficits, neuron loss, and reduced anxiety coinciding with axonal degeneration and intraneuronal Abeta aggregation in the 5XFAD mouse model of Alzheimer's disease. Neurobiol. Aging 33 (196), e29–e40.
Kellogg, C.M., et al., 2023. Microglial MHC-I induction with aging and Alzheimer's is conserved in mouse models and humans. Geroscience. 45, 3019–3043.
Kim, K., et al., 2021. Therapeutic B-cell depletion reverses progression of Alzheimer's disease. Nat. Commun. 12, 2185.
Laurent, C., et al., 2017. Hippocampal T cell infiltration promotes neuroinflammation and cognitive decline in a mouse model of tauopathy. Brain 140, 184–200.
Lee-Chang, C., et al., 2014. Accumulation of 4–1BBL+ B cells in the elderly induces the generation of granzyme-B+ CD8+ T cells with potential antitumor activity. Blood 191, 4141–4151.

Lee-Chang, C., et al., 2016. Aging Converts Innate B1a Cells into Potent CD8+ T Cell Inducers. J. Immunol. 196, 3385–3397.
Li, J., et al., 2022. KIR(+)CD8(+) T cells suppress pathogenic T cells and are active in autoimmune diseases and COVID-19. Science 376, eabi9591.
Machhi, J., et al., 2021. CD4+ effector T cells accelerate Alzheimer's disease in mice. J. Neuroinflammation 18, 272.
Marsh, S.E., et al., 2016. The adaptive immune system restrains Alzheimer's disease pathogenesis by modulating microglial function. PNAS 113, E1316–E1325.
Mattson, M.P., 2004. Pathways towards and away from Alzheimer's disease. Nature 430, 631–639.
Meda, L., et al., 1995. Activation of microglial cells by beta-amyloid protein and interferon-gamma. Nature 374, 647–650.
Monsonego, A., et al., 2003. Increased T cell reactivity to amyloid beta protein in older humans and patients with Alzheimer disease. J. Clin. Invest. 112, 415–422.
Nicoll, J.A., et al., 2003. Neuropathology of human Alzheimer disease after immunization with amyloid-beta peptide: a case report. Nat. Med. 9, 448–452.
Oakley, H., et al., 2006. Intraneuronal beta-amyloid aggregates, neurodegeneration, and neuron loss in transgenic mice with five familial Alzheimer's disease mutations: potential factors in amyloid plaque formation. J. Neurosci. 26, 10129–10140.
Olkhanud, P.B., et al., 2012. DNA immunization with HBsAg-based particles expressing a B cell epitope of amyloid beta-peptide attenuates disease progression and prolongs survival in a mouse model of Alzheimer's disease. Vaccine 30, 1650–1658.
Orgogozo, J.M., et al., 2003. Subacute meningoencephalitis in a subset of patients with AD after Abeta42 immunization. Neurology 61, 46–54.
Ortiz, B.D., Nelson, P.J., Krensky, A.M., 1997. Switching gears during T-cell maturation: RANTES and late transcription. Immunol. Today 18, 468–471.
Pardi, N., et al., 2015. Expression kinetics of nucleoside-modified mRNA delivered in lipid nanoparticles to mice by various routes. J. Control. Release 217, 345–351.
Pernold, K., et al., 2019. Towards large scale automated cage monitoring - Diurnal rhythm and impact of interventions on in-cage activity of C57BL/6J mice recorded 24/7 with a non-disrupting capacitive-based technique. PLoS One 14, e0211063.
Piehl, N., et al., 2022. Cerebrospinal fluid immune dysregulation during healthy brain aging and cognitive impairment. Cell 185 (5028–5039), e13.
Poon, C.H., et al., 2023. Sex Differences between Neuronal Loss and the Early Onset of Amyloid Deposits and Behavioral Consequences in 5xFAD Transgenic Mouse as a Model for Alzheimer's Disease. Cells. 12.
Prinz, M., Priller, J., 2014. Microglia and brain macrophages in the molecular age: from origin to neuropsychiatric disease. Nat. Rev. Neurosci. 15, 300–312.
Rosset, M.B., et al., 2015. Vaccine-induced Abeta-specific CD8+ T cells do not trigger autoimmune neuroinflammation in a murine model of Alzheimer's disease. J. Neuroinflammation 12, 95.
Sanchez-Molina, P., et al., 2022. Chronic IL-10 overproduction disrupts microglia-neuron dialogue similar to aging, resulting in impaired hippocampal neurogenesis and spatial memory. Brain Behav. Immun. 101, 231–245.
Schupf, N., et al., 2008. Peripheral Abeta subspecies as risk biomarkers of Alzheimer's disease. PNAS 105, 14052–14057.
Smith, L.K., et al., 2015. beta2-microglobulin is a systemic pro-aging factor that impairs cognitive function and neurogenesis. Nat. Med. 21, 932–937.
Smolders, J., et al., 2013. Characteristics of differentiated CD8(+) and CD4 (+) T cells present in the human brain. Acta Neuropathol. 126, 525–535.
Smolders, J., et al., 2018. Tissue-resident memory T cells populate the human brain. Nat. Commun. 9, 4593.
Spani, C., et al., 2015. Reduced beta-amyloid pathology in an APP transgenic mouse model of Alzheimer's disease lacking functional B and T cells. Acta Neuropathol. Commun. 3, 71.
St-Amour, I., et al., 2013. Brain bioavailability of human intravenous immunoglobulin and its transport through the murine blood-brain barrier. J. Cereb. Blood Flow Metab. 33, 1983–1992.
Stern, J.N., et al., 2014. B cells populating the multiple sclerosis brain mature in the draining cervical lymph nodes. Sci. Transl. Med. 6, 248ra107.
Su, W., et al., 2023. CXCR6 orchestrates brain CD8(+) T cell residency and limits mouse Alzheimer's disease pathology. Nat. Immunol. 24, 1735–1747.
Unger, M.S., et al., 2020. CD8(+) T-cells infiltrate Alzheimer's disease brains and regulate neuronal- and synapse-related gene expression in APP-PS1 transgenic mice. Brain Behav. Immun. 89, 67–86.
van Dyck, C.H., et al., 2023. Lecanemab in Early Alzheimer's Disease. N. Engl. J. Med. 388, 9–21.
VanGuilder Starkey, H.D., et al., 2012. Neuroglial expression of the MHCI pathway and PirB receptor is upregulated in the hippocampus with advanced aging. J. Mol. Neurosci. 48, 111–126.
Walzer, T., et al., 2003. Cutting edge: immediate RANTES secretion by resting memory CD8 T cells following antigenic stimulation. J. Immunol. 170, 1615–1619.
Yousef, H., et al., 2019. Aged blood impairs hippocampal neural precursor activity and activates microglia via brain endothelial cell VCAM1. Nat. Med. 25, 988–1000.
Zenaro, E., et al., 2015. Neutrophils promote Alzheimer's disease-like pathology and cognitive decline via LFA-1 integrin. Nat. Med. 21, 880–886.
Zhan, X., et al., 2015. Myelin basic protein associates with AbetaPP, Abeta1-42, and amyloid plaques in cortex of Alzheimer's disease brain. J. Alzheimers Dis. 44, 1213–1229.
Zhang, P., et al., 2019. Senolytic therapy alleviates Abeta-associated oligodendrocyte progenitor cell senescence and cognitive deficits in an Alzheimer's disease model. Nat. Neurosci. 22, 719–728.